Nanofiber Cellulose Grafted with Lauric Acid as a New Phase Change Material (PCM) used in Buildings for Thermal Energy Storage

Soumaya Zormati[1], Fadhel Aloulou[1,a)], Habib Sammouda[1]

[1]University of Sousse, Laboratory of Energy and Materials (LabEM-LR11ES34), Higher School of Science and Technology of Hammam Sousse, Street LamineAbbassi 4011Hammam Sousse, Tunisia

[a)]Address all correspondence to this author. e-mail: alouloufadhel@gmail.com, ORCID: 0000-0002-6586-2328.

Abstract:

In this research, Cellulose Nanofibers (NFC) modified with a eutectic of lauric acid (LA) was prepared as a new form-stable phase change material (NFC-LA). Thermal properties of this composite were investigated by Differential Scanning Calorimetry (DSC). The results revealed that the melting temperature and latent heat of NFC/LA were 21.56 °C and 88.5 J/g, respectively; and the super cooling degree for the NFC-LA composite decreased to 13.99 °C when compared to 20.28 °C of the pure lauric acid. Natural clay was purified and modified with Cetyltrimethyl ammonium bromide (CTAB) to prepare organoclay. Through FTIR spectra, we have confirmed that the clay was successfully modified. The PCM-composite was then added to the organoclay to obtain a new composite denoted NFC-LA-OC. this latter was added to cement and was investigated as a reinforcement material in cement mortars for thermal energy storage application. The prepared material can both solve the leakage problem associated to the phase change material, and reduce or even avoid the use of heating and air conditioning systems, which are energy-intensive systems, and therefore reduce energy consumption.

Keywords: Cellulose Nanofiber, Organoclay, PCM, Thermal Energy Storage, Building, Composite materials**.**

 doi:10.20944/preprints202204.0148.v1

1. Introduction

Today the management of buildings energy demand, and the search for new solutions to integrate into the renovation process is an essential step to achieve energy efficiency. In the context of sustainable development, the new regulations on thermal insulation in the building sector encourage the development of new bio-based materials for the construction of energy-efficient buildings while ensuring home comfort [1-3]. However, to ensure better insulation in construction materials, it is necessary to combine a poorly conductive material with either cement or other construction materials. Insulators of composite structures are either placed inside or as barrier elements of the materials of the supporting structure, such as mineral insulators, fibers and glass wool, rock wool, expanded perlite, or bio-organic insulating type and plants, flax fibers, hemp fibers, coconut fibers, straw, sheep's wool, feathers, or of synthetic insulation type, expanded or extruded polystyrene, polyurethane [4-6].

Among the multiple thermal insulation methods in the building industry, silicaparticlesfoam has also been used to fabricate concrete structures with good thermal performance [7,8]. Improved nanocomposite concrete is obtained by incorporating silica particles foam into a high strength cement matrix, combining the advantages of conventional concrete (compressive strength, moldability) with the properties of thermal insulation material. Silica particles foam incorporated in ordinary concrete has also shown great performance in terms of mechanical and thermal properties [9-11]. Other studies have shown that the silica particles foamincorporatedin concrete has excellent sound insulation and excellent fire resistance [9,13]. However, despite it having a very low thermal conductivity and a super-insulating character, silica particles foam has some major drawbacks substantially its high cost, fragility and toxicity. To overcome these deficiencies, a new research axis has recently been carried out with the aim of developing bio-sourced and super-insulating composite materials. Thus composites based on cellulose or its derivatives, or other polysaccharides have been investigated [14-17]. Modified cellulose nanofiber or its derivatives can be an innovative solution for manufacturing high added value biomaterials, especially in the thermal insulation industry [18-20].

Due to the enormous energy consumption of buildings related to heating and cooling indoor spaces, different works focused lately on developing new building materials having alluring mechanical and thermal insulating characteristics. However, the improvement of the mechanical properties leads generally to deterioration in the overall thermal insulation performance.

 doi:10.20944/preprints202204.0148.v1

The thermal performance of the building wall coatings is a key factor in determining the measure of the energy required for the comfort of nature. In this regard, a few examinations consider the reason that energy consumption can be improved by joining thermal insulation materials in to walls and roofs [20,21]. Thermal insulation can be considered as the ability of a material to ease back or to slow the heat flow inside or outside the building. Currently, the research of bio-based materials, using natural fibers or clay, has increased to be used to reinforce cementitious materials, that works to enhance the mechanical properties of the cementitious material generally by accelerating the formation and the precipitation of hydration products [14,15,22]. In this sense, numerous scientists investigated clay, which belongs to the phyllo silicate family, was due to the permeable media, in exchange, it could also be mixed with many fibers considered as a material with a wide range of applications. The example of clay-based materials was selected. In which case, there is good reason to use modified clay such as chlorite, Kaolinite and Illite, which are considered as filler in the composite material, to enhance the properties of cement thanks to its low cost, availability and its excellent characteristics [18]. Besides, in many studies, it was remarkable to note that the role of organoclay has gained many interests in both academic and industrial research [12] due to the excellent performance as well as the way to modify, to as clay-based composite [13]. It's important to mention that natural fibers have grown to develop environmental-friendly construction materials. These fibers are biodegradable, lighter and abundant resources like sisal, Flax, Hemp, Bamboo, coir and others [19,23].

The main objective of this work is to elaborate a new ecological and bio-based nanocomposite as an intelligent material for implementation in the building sector. The idea is therefore to develop new energy-storage material, to be usedas wall coatings in buildings,allowing the storageand transfer of thermal energy and therefore to minimize energy consumption. Subsequently, Cellulose Nanofibers (NFC) were modified with a eutectic lauric acid (LA), and then dispersed in organophilic clay (OC). The prepared material can both solve the leakage problem associated to the phase change material, and reduce or even avoid the use of heating and air conditioning systems, which are energy-intensive systems, and therefore reduce energy consumption.

Fourier Transform Infrared (FTIR) spectroscopy, ^{13}C CP-MAS NMR spectroscopy, X-ray diffraction (XRD), leakage test, Differential Scanning Calorimetry (DSC) and thermal conductivity are the different techniques used in this work to characterize the elaborated composite alongside the other materials.

 doi:10.20944/preprints202204.0148.v1

2. Materials and Methods:

2.1 Materials

The clay used in this work is natural clay from Jemmel city (Tunisia). The CTAB is a cationic surfactant (M_w= 336.39g mol^{-1}), a quaternary alkyl ammonium salt soluble in H_2O and used in the preparation of OC. The SDBS (M_w= 348.48 g mol^{-1}) is sodium dodecylbenzenesulfonate, an anionic surfactant used in the fabrication of composites. The used Lauric acid was from coconut oil.

2.2 Treatment of natural clay

The natural clay has initially undergone a purification step where it was washed with distilled water to eliminate impurities. Then, 500 g of clay was attacked with sulfuric acid; it was dispersed in a volume of 1L of sulfuric acid (2M) and was kept under continuous stirring at 80°C until complete dispersion. The treated clay was rinsed several times with distilled water and filtered until pH became 7. Finally, it was dried at 105°C for 24h and crushed with a mortar.

2.3 Preparation of organoclay (OC)

The organoclay (OC) was synthesized by intercalation of CTAB, a quaternary alkyl ammonium salt, between the layers of the clay by a simple cationic exchange. The primary goal of CTAB intercalation is to increase the interlayer spacing and reduce the secondary bonding attractions between the clay platelets. Different studies have shown that this surfactant intercalation could not only increase the clay interlayer basal spacing but also change the hydrophilic character of the natural clay surface [21]. Thus, a solution of 1 L of hydrochloric acid (10^{-2} M) was introduced in an Erlenmeyer of 1L and it was carried to a temperature of 80°C before slowly introducing 10^{-3} moles of CTAB. It was maintained under constant stirring at 80°C for 3 hours. Then, 10 g of clay was added to the solution and was kept under continuous stirring at the same temperature for another 3 hours. Finally, the clay was washed several times with distilled water and filtered to eliminate the inorganic cations, and then dried at 80°C.

2.4 Sample Preparation

The phase change material was trapped by the carrier polymer using an oil-in-water emulsion, a solvent evaporation method. 200 mg of cellulose nanofiber modified by grafting lauric acid were dispersed in 5 ml dichloromethane. The organic phase obtained was poured in 20 ml of distilled water containing 2% SDBS surfactant as an emulsifier, and was stirred magnetically for 3 hours at 800 rpm under atmospheric pressure at

Preprints (www.preprints.org) | NOT PEER-REVIEWED | Posted: 15 April 2022 doi:10.20944/preprints202204.0148.v1

room temperature to remove the organic solvent. The mixture obtained is called NFC-LA. The composite pastes were mixed in a specified mixer and they were prepared by incorporating 35%, 45%, 50%, 55%, 60% and 65% of organophilic clay adding to each mortar different NFC-LA percentage of 60%, 50%, 45%, 40%, 35% and 30% by weight of organophilic clay (Table 1). To ensure the dispersion of the NFC-LA in the organophilic clay, the NFC-LA gel was premixed with a solution of an anionic surfactant of concentration at the critical micellar concentration (CMC of SDBS) for 5 minutes using a mixer until the complete dispersion of the modified nanofiber. After the mixing procedure, cylindrical molds with a cross-section of 10 mm and a height of 2 mm were prepared for each mixture. After 24 h, the samples were unmolded and cured at 95% relative humidity and 23.0 °C ± 2.0 °C before the test days (Fig. 1).

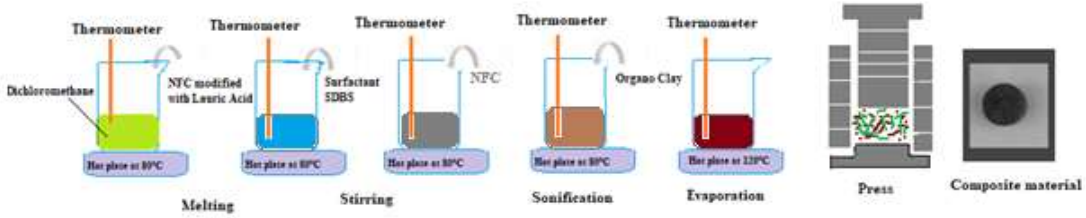

Fig. 1. The process of preparing the composite material

Table1 : The composition of the Lauric acid/NFC/Organo-Clay composites

Samples	E1	E2	E3	E4	E5
% Lauric Acid	60	50	45	35	30
%NFC	5	5	5	5	5
% Organo-Clay	35	45	50	60	65

2.5 Characterization

The composite was characterized by Fourier transform infrared (FTIR) spectroscopy, differential scanning calorimetry (DSC) and thermal conductivity. In addition, OC in powder form was characterized by structural X-ray diffraction.

2.5.1 X-ray diffraction (XRD)

The XRD pattern was measured with an X-ray diffractometer in the 2Θ range between 5° and 80°, using CuKα; (γ=1.54060Å) radiation at 40 kV and 30 mA. With exceptional analysis speed, with a step size of 0.02°/s, a

Preprints (www.preprints.org) | NOT PEER-REVIEWED | Posted: 15 April 2022 doi:10.20944/preprints202204.0148.v1

collection time of 40s per step, and an angle of incidence of 1°. The crystallization rate is calculated from the intensity of the crystalline and amorphous curve of the XRD profile. X-ray measurements were performed on powdered samples after the organophilic clay (OC) had been air-dried.

2.5.2 Fourier transform infrared (FTIR) spectroscopy

The Fourier transform infrared (FTIR) spectroscopy was used to analyze the composition of the NFC before and after modification with LA. FTIR spectrum was obtained from KBr pellets with a Perkin Elmer spectrometer used in transmission mode in the range of 400-4000 $cm^{-1}$with a resolution of 2 cm^{-1}.

2.5.3 Analysis of Thermal Properties by (DSC) Differential Scanning Calorimetry

The latent heat and phase change temperature of lauric acid from coconut oil and PCM composite were measured using a differential scanning calorimeter (Perkin Elmer DSC 4000). The temperature range was -20°C to 100°C, with a heating and cooling rate of 10°C/min under the high purity nitrogen shielding gas (99.99% purity).

2.5.4 Thermal conductivity

The thermal conductivity of all samples was calculated by a transient plane heat source method using the hot disk thermal constant analyzer (TPS 2500 S).

3 Results and discussion

3.1 Characterization of modified fibers

The modified nanofibrillated cellulose used in this study was obtained by heterogeneous esterification with linear lauric acid at a degree of substitution level of 0.3. The modified nanofibrillated cellulose fibers were analyzed by FTIR and solid-state ^{13}C NMR.

FTIR spectra (Fig. 2) exhibited the presence of ester carboxyl absorption band at 1740 cm^{-1}, methylene peak at 2850 cm^{-1} and 1540 cm^{-1}.

Preprints (www.preprints.org) | NOT PEER-REVIEWED | Posted: 15 April 2022 doi:10.20944/preprints202204.0148.v1

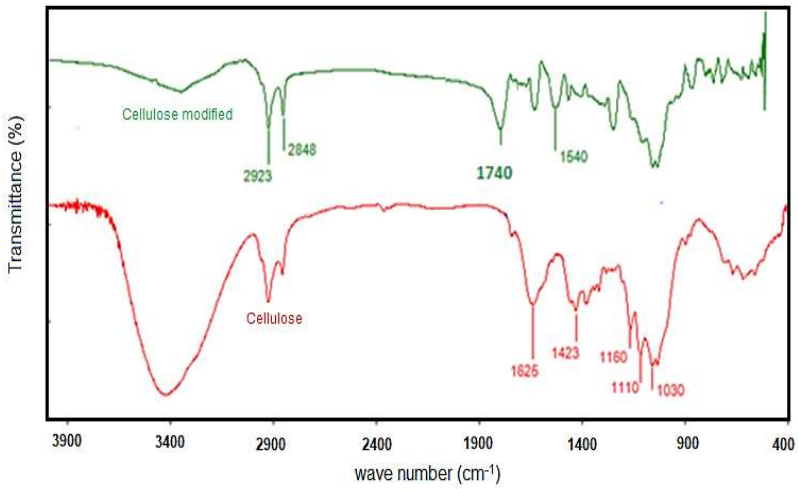

Fig.2. FTIR spectra of cellulose fiber (NFC) and the modified one after esterification with Lauric acid at DS=0.3

The ^{13}C NMR spectrum of the cellulose fiber presented in Fig. 3 shows that the signals at 104.7 ppm (C-1), 89.8 ppm (C-4), 74.7 ppm (C-5), 72 ppm (C-2 and C- 3) and that at 69.5 ppm (C-6), are assigned to six carbon atoms of the glucose unit. The signals, appearing in the spectrum of modified cellulose fibers at 173.8 ppm, are assigned to the carbon atoms of the C-7 carboxylic groups and the signal at 15-40 ppm is assigned to the methylene carbon.

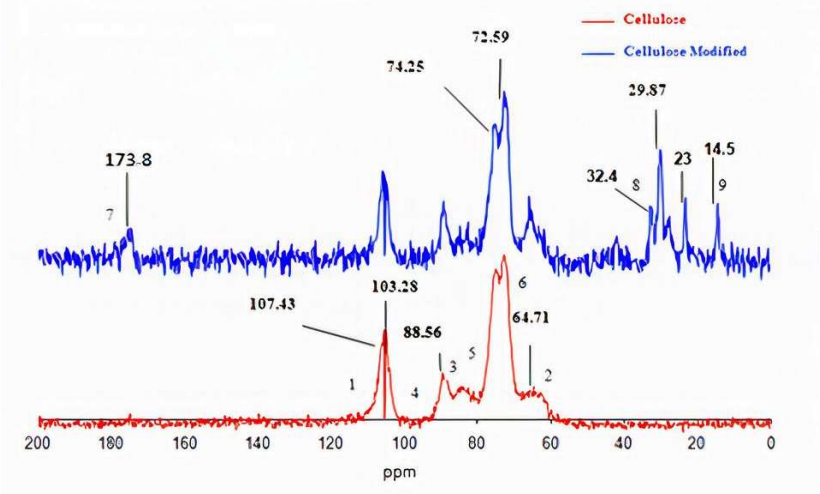

Fig. 3. CP MAS ^{13}C MNR spectra of native cellulose fiber (NFC) and the modified one after esterification with lauric acid at DS=0.3

3.2 Characterization of OC

3.2.1 Characterization by XRD

Fig.4. shows the XRD patterns of natural clay and organo modified clay. The XRD pattern of natural clay (Fig.3.) shows the presence of typical montmorillonite reflections (2θ = 6.8° ; 20.02° ; 36.64° and 61.98°). Other peaks also exist in the XRD pattern which correspond to trace impurities such as quartz (2θ = 21.02° and 26.88°) and feldspar (2θ =27.52°). A significant change in the diffraction pattern appears after clay modification with

Preprints (www.preprints.org) | NOT PEER-REVIEWED | Posted: 15 April 2022 doi:10.20944/preprints202204.0148.v1

CTAB. The shift of the main diffraction peak at 6.8° to 5.28° shows the effects of the organophilic treatment. This shift indicates an increase of the inter planar spacing d_{001} from 1,305 nm (2θ =6.8°) to 1.674 nm (2θ =5.28°) confirming the intercalation of CTAB between the clay layers.

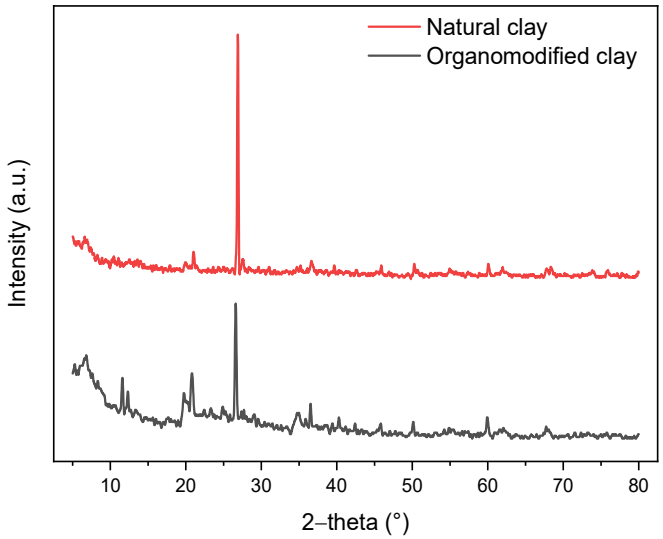

Fig.4. XRD patterns of natural and organo modified clay (clay modified with CTAB)

3.2.2 Infrared spectral characteristics of organoclay

In the FTIR spectra of pure clay and of clay treated with H_2SO_4 and clay modified with CTAB (Fig.5), the band at 3620-3390 cm^{-1} presented an OH stretching vibration. The treatment of clay with the CTAB led to the appearance of two peaks at 2920 $cm^{-1}$and 2851 cm^{-1} assigned to the symmetrical stretching vibration and asymmetrical elongation of CH_2 groups from the organic chain of the quaternary ammonium salt incorporated into clay.The CH_2 bending vibration mode was inferred by the peak at 1470 cm^{-1}, confirming the existence of quaternary ammonium ions in the clay interlayer space [24]. The bond OH (1628 cm^{-1}) corresponds to water molecules adsorbed on the clay surface [25] (Fig.4). The band at 3420 cm^{-1} is attributed to the internal hydroxyls linked to aluminum. Similar results have been reported in the literature [23].

In the 2000-500 cm^{-1} range, the raw and modified clay spectra reveal several characteristic absorption bands. The band at 1032 cm^{-1} confirms the existence of Si-O-Si bonds in crude clay. We note that the clay is known by the appearance of a peak at 3621 cm^{-1} and shoulders at 3680 and 3345 cm^{-1}. This peak is particularly characteristic of clay and corresponds to the stretching vibration of elongation of the OH groups of the octahedral layer band associated with the Si-O-Si stretching vibration of clay. The peaks at 1428 cm^{-1} and 3420 cm^{-1} are attributed to the presence of O-H stretching vibration.

Preprints (www.preprints.org) | NOT PEER-REVIEWED | Posted: 15 April 2022 doi:10.20944/preprints202204.0148.v1

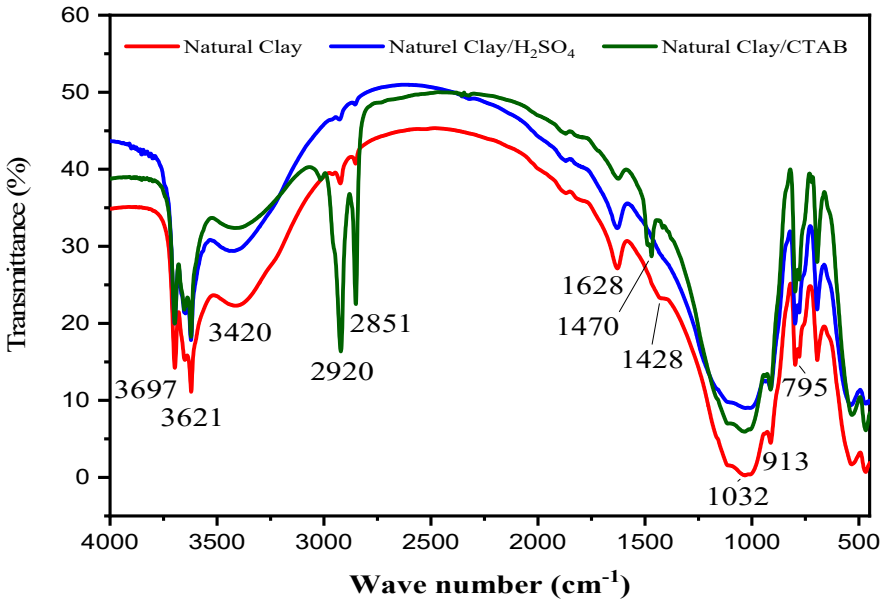

Fig.5.FTIR spectra of natural clay, natural clay treated withH_2SO_4andclay modified with CTAB (OC)

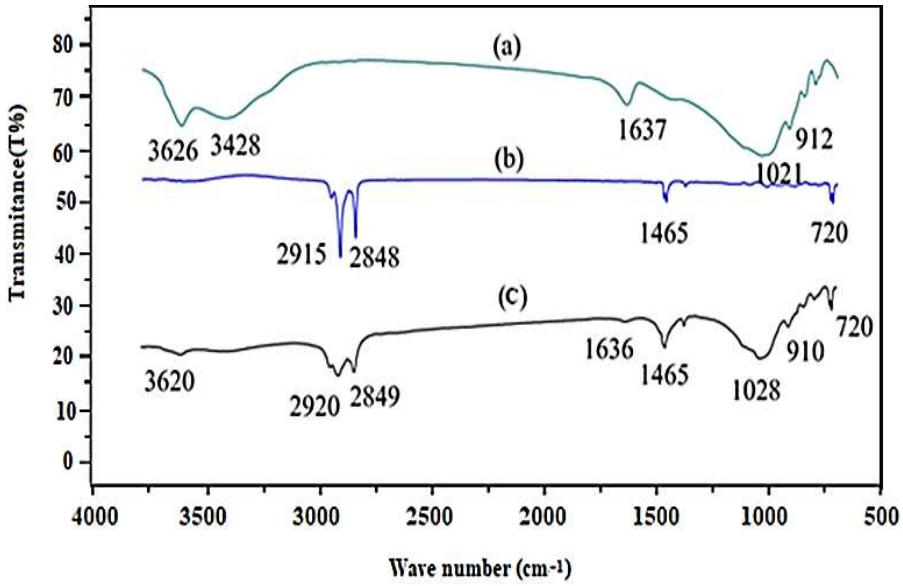

Fig.6.FTIR spectra of (a)NFC/Organoclay, (b)Lauric Acid and(c) NFC/Organoclay/Lauric Acid

In Fig.6(a), the intermolecular OH groups resulting from their OC stretching vibrations were located at approximately 3626 and 3428 cm^{-1}. The peak at 1637cm^{-1} was the absorption of bending vibrations of OH groups in OC. The peaks at 1021 and 912cm^{-1} in OC were the asymmetric stretch vibration of Si-O-Si and the bending vibrations in the plane of Si-O. The intermolecular stretch vibration OH groups switched at around 3621 and 3428 cm^{-1} got a little wider, smaller, but still clearly existed. He indicated that there were inorganic cations in the layered silicates. However, these peaks have widened and some have almost disappeared. These

 doi:10.20944/preprints202204.0148.v1

phenomena indicated that the number of OH groups was reduced and that the structure of the clay was successfully converted from hydrophilic to organophilic. However, there were two peaks with small changes, which indicated that the lamellar structure of the clay was not changed and had better energy storage stability (Fig. 6(c)). In addition, the peak at 1021 cm^{-1} shifted to a longer wavelength and became narrow and intensive. This showed a closer combination with the widened spacing between layers in the structure of this organic clay. These results were consistent with XRD analysis. There are four major peaks in the FTIR spectrum of pure LA (Fig. 6(b)). The peaks at 2915 and 2848 cm^{-1} were attributed to asymmetric and symmetrical stretching vibrations of C-H. These peaks became wider and increased. The reasons for these changes resulted from the successful intercalation of modified nanofibrillated cellulose with lauric acid molecules into the organophilic clay. This confirms the incorporation of LA molecules between the silicate layers. In addition, the other two peaks at 1465 and 720 cm^{-1} were related to the CH_2 or CH_3 strain vibration and the CH_2 flip-flop vibration in $(CH_2)_n$. In addition, two characteristic peaks of LA also existed in the FTIR spectra of NFC-LA-OC composite. This showed that the structure of the paraffin was not changed and confirmed that these two types of clay minerals are still a type of PCM.

3.3 Physical, chemical and thermal properties

3.3.1 PCM leak test

The form-stable property of the phase change material is an important factor for practical thermal storage applications. Therefore, it is necessary to carry out a leakage test of pure lauric acid and of the prepared PCMs composites. All the samples were prepared in the form of cylindrical pellets and then the leakage test was carried out by introducing the pellets into laboratory oven on filter paper at 100°C for 1 hour (Fig. 7-a).

After heating at 100°C for 1 h, the samples were examined. The sample S_0 (pure lauric acid) completely melted into liquid. The composite S_1 which was made by dispersing 0.15wt% OC with LA/NFC composite particles showed obvious material leakage. The sample S_2, which was prepared by dispersing 0.5 wt% OC with LA/NFC, showed that a big part of the PCM absorbed melted onto the filter paper, leaving a stain on the filter paper. The S_3 composite was prepared by dispersing 1wt% OC with LA/NFC and it has exhibited slight leakage. The sample S_4 produced by dispersing 1.5 wt% OC with LA/NFC retained in its original shape with little leakage. However, for the sample S_5, which was produced by dispersing 2 wt% OC with the LA/ NFC, there was no leakage observed (Fig. 7-b). The results show that the shape stabilization of the S_5 composite material is due to the robust physical interaction between LA and the porous network interconnection between the NFC and the OC sheets. The mass and structure of the material remained constant during the heating process, due to the good

Preprints (www.preprints.org) | NOT PEER-REVIEWED | Posted: 15 April 2022 doi:10.20944/preprints202204.0148.v1

mechanical integrity and porous morphology of the added compounds. In addition, LA is easily absorbed into the porous structures of NFC/OC due to the strong capillary force and surface tension.

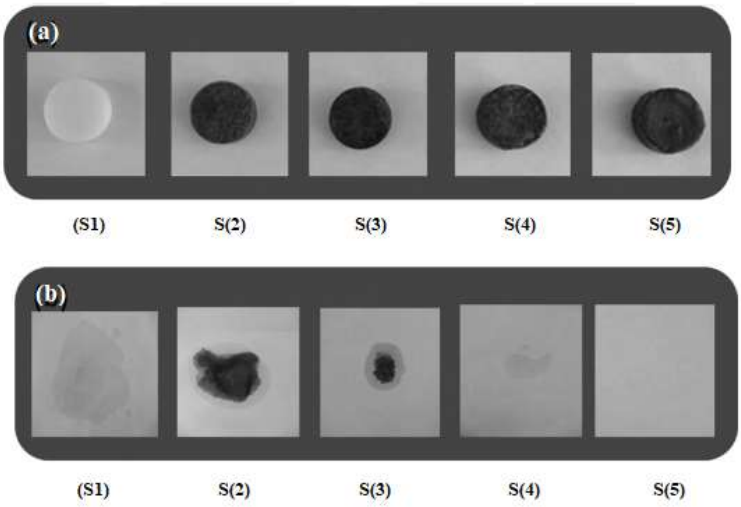

Fig. 7. Leakage test of NFC-LA wax and different composite materials: (a) before heating, (b) after heating at temperature 100 °C.

In the following part, a thermal analysis of the sample $S_5$was realized using Differential Scanning Calorimetry (DSC).

3.3.2 Analysis of Thermal Properties by Differential Scanning Calorimetry (DSC)

Differential Scanning Calorimetry (DSC) was performed to determine the thermal energy storage characteristics of pure PCM and those of prepared PCMComposite. Indeed, the melting temperature and the latent heat capacity are crucial parameters to define the PCM or PCMcomposite as materials intended for the storage of energy used in the building.

Therefore, the PCMcomposite material, to be incorporated into the building material and more precisely into the wall, must have a well-suited phase transition temperature as well as a fairly high enthalpy. Fig.8(a) shows the DSC thermogram of pure PCM (Lauric Acid). An endothermic signal (during heating) and another exothermic (during cooling) are observed with a heating or cooling rate of 5°C/min.The peak of the first signal, corresponding to the solid-liquid phase transition of PCM occurs at a temperature of 23.53°C (melting temperature) and a latent heat capacity of 90.1 J/g. From the exothermic signal, a solidification temperature of 3.25 °C and a latent heat capacity of 91.8 J/g are determined.

Preprints (www.preprints.org) | NOT PEER-REVIEWED | Posted: 15 April 2022 doi:10.20944/preprints202204.0148.v1

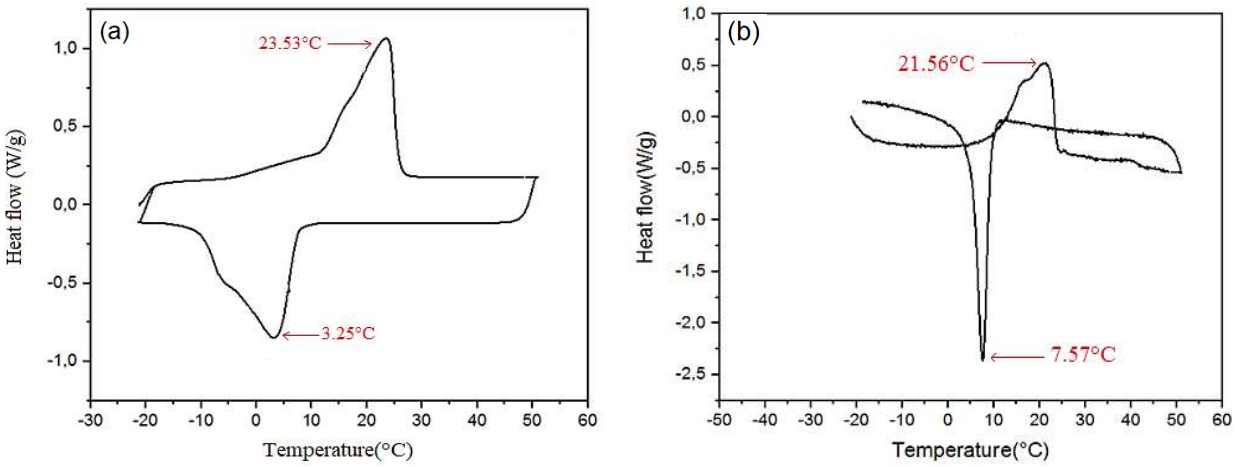

Fig.8.DSC Curves of (a)Lauric Acid and (b) PCM-composite

Comparing the melting and cooling temperatures obtained with the literature, we see a significant difference for the solidification temperature which is 17.44 °C. Many studieshave shown that the rate of heating and cooling acts directly on the specters by shifting the peaks of phase transitions.

The thermal energy storage property of the PCM-composite sample is illustrated in Fig.8(b). The solid-liquid phase transition takes place at a melting temperature of 21.56 °C and with a heat capacity of 88.5 J/g. While the solidification temperature and heat capacities are 7.57 °C and 87.64 J/g respectively.

From the Table 2, we can notice that the Latent heat of PCM fell to lower values after its incorporation, while their melting point and solidification points remained almost constant.

However, the prepared sample has good thermal energy storage performance (latent heat of fusion and significant solidification) and no PCM leakage is observed. This makes these composites good candidates for energy storage in buildings.

Table 2. Thermal properties of Lauric Acid and the prepared composite

PCM-composite	Melting point T_m (°C)	Solidification Temperature T_c (°C)	Latent heat of fusion (J/g)	Latent heat of solidification (J/g)
Lauric Acid	23.53	3.25	90.098	91.78
Elaborated Composite	21.56	7.57	88.5	87.64

Preprints (www.preprints.org) | NOT PEER-REVIEWED | Posted: 15 April 2022 doi:10.20944/preprints202204.0148.v1

In Fig.9, we represented the superposition of the DSC spectra of the composite with that of lauric acid.

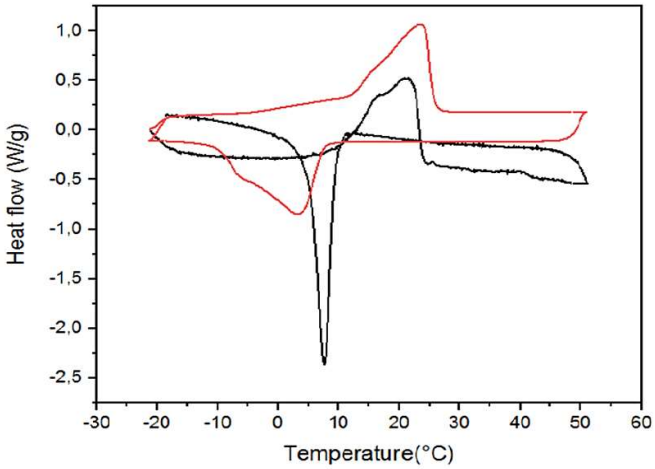

Fig.9. DSC image of pure PCM and PCM-composite

We calculated the PCM encapsulation ratio by the following formula from the DSC analysis:

$$R = \frac{\Delta \mathrm{Hm}(\mathrm{PCM}_{\mathrm{composite}})}{\Delta Hm(PCMpure)} \times 100\%$$

We note that the prepared material, already having the highest thermal capacity, has a very high degree of encapsulation of 98.2%.

We made a comparison of our results with those found in the literature relating to thermal characteristics of PCM similar to our work (Table 3).

Table 3. Comparative table of thermal properties of the prepared composite and other composites

PCM-composite	Melting point T_m (°C)	Solidification Temperature T_c(°C)	Latent heat (J/g)	Ref
Elaborated composite	21.5	7.5	87.6	Our work
RT20/clay composite	23	23	79.25	[26]
Coconut oil impregnated biochar	24.85	-	74.6	[27]
Wood Flour/Lauric Acid-Myristic Acid	33.1	32.6	60.5	[28]
Palm Oil/Cellulose/Clay/ graphite	27.3	27	41.1	[12]

Preprints (www.preprints.org) | NOT PEER-REVIEWED | Posted: 15 April 2022 doi:10.20944/preprints202204.0148.v1

3.3.3 Thermal conductivity

An interesting part in this work focused on the study of the thermal behavior of the materials produced. Table 4 presents thermal conductivity of different PCM composites (S_1, S_2, S_3, S_4, S_5) as well as pure PCM (S_0). An improvement in the thermal conductivity of PCM composite samples compared to the pure LA, and proportionally to the added percentages of OC, was remarked. The increase in thermal conductivity reached 60% (Fig. 10).

The obtained results proves that the sample S_5 has an optimal thermal performance thanks to the thermal stability of the prepared material,thatmake it a promising material for thermal energy storage and energy managementin buildings.

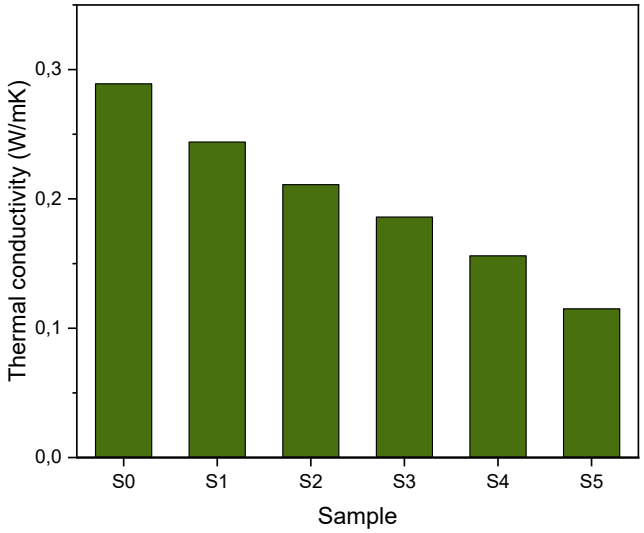

Fig.10. Thermal conductivity of different PCM composites

Table 4. Thermal conductivity of different composites samples

NFC-LAadded rate (%)	Samples	Thermal Conductivity (W/mK)	Decrease in thermal conductivity (%)
0	S_0	0.289	-
0.5	S_1	0.244	41.94
1	S_2	0.211	49.05
1.5	S_3	0.186	49.78
2	S_4	0.156	55.58
5	S_5	0.115	58.05

 doi:10.20944/preprints202204.0148.v1

4 Conclusion

In this study, PCMs of organic clays were prepared by two-step intercalation; the first was ion exchange intercalation of organophilic clays with the CTAB surfactant, then a secondary hydrophobic attractive force forlauric acid (LA) grafted onto the cellulose nanofibers (NFC) occurred. The clay spacing changed accordingly, expanding in organic clays after intercalation of CTAB and then to a higher intercalation spacing after absorbing NFC/LA in the clay galleries.

The Cellulose Nanofiber/lauric acid/Organophilic-clay (NFC/LA/OC) composition was suitable for a phase change material which remained in the solid state without any liquid leakage, even when heated to a temperature above the melting point of lauric acid.

Thermal stability and thermal behaviour of lauric acid composites were studied by DSC. The data of DSC analysis indicated that organophilic-clay (OC) greatly improved thermal stability.

TheNFC/LA/OC material is considered to be a new energy storage material or PCM to absorb and release heat according to the change in environmental temperature.

The sample prepared by anionic surfactant emulsion (SDBS), dispersing the nanofibers evenly and minimizing the pore size of the material. The latent thermal capacity obtained has a fairly large thermal storage potential in the building envelopes. Indeed, it can retain up to 98.25% by weight of lauric acid fat without having any leakage phenomenon because it has good thermal stability characteristics, the measurement of the thermal conductivity of the PCM composite was between 0.298 W/mK and 0.115 W/mK.

 doi:10.20944/preprints202204.0148.v1

Authors' contributions: All authors contributed to the study conception and design. Material preparation, data collection and analysis were performed by Soumaya Zormati and Fadhel Aloulou. The first draft of the manuscript was written by Fadhel Aloulou. Habib Sammouda and Fadhel Aloulou commented on previous versions of the manuscript. All authors read and approved the final manuscript.

Funding: The authors did not receive support from any organization for the submitted work.

Conflict of interest: The authors have no conflicts of interest to declare that are relevant to the content of this article.

Data availability: The data used to support the findings of this study are available from the corresponding author upon request. The datasets analysed during the current study are available from the corresponding author on reasonable request.

Code availability: not applicable

References

1. S. R. L. da Cunha and J. L. B. de Aguiar, J. Energy Storage **27**, 101083 (2020).

2. B. Abu-Jdayil, A. H. Mourad, W. Hittini, M. Hassan, and S. Hameedi, Constr. Build. Mater. **214**, 709 (2019).

3. L. Belussi, B. Barozzi, A. Bellazzi, L. Danza, A. Devitofrancesco, C. Fanciulli, M. Ghellere, G. Guazzi, I. Meroni, F. Salamone, F. Scamoni, and C. Scrosati, J. Build. Eng. **25**, 100772 (2019).

4. S. Burhenne, O. Tsvetkova, D. Jacob, G. P. Henze, and A. Wagner, Build. Environ. **62**, 143 (2013).

5. P. Das, L. Van Gelder, H. Janssen, and S. Roels, J. Build. Perform. Simul. **10**, 3 (2017).

6. Q. Zeng, T. Mao, H. Li, and Y. Peng, Energy Build. **174**, 97 (2018).

7. L. Ratke, Beton- Und Stahlbetonbau **103**, 236 (2008).

8. S. Kim, J. Seo, J. Cha, and S. Kim, Constr. Build. Mater. **40**, 501 (2013).

9. A. C. Pierre and A. Rigacci, in *Aerogels Handb.*, edited by M. A. Aegerter, N. Leventis, and M. M. Koebel (2011), pp. 21–45.

10. A. Hub, G. Zimmermann, and J. Knippers, Beton- Und Stahlbetonbau **108**, 654 (2013).

11. Y. K. Akimov, Instruments Exp. Tech. **46**, 287 (2003).

12. L. Boussaba, S. Makhlouf, A. Foufa, G. Lefebvre, and L. Royon, J. Build. Eng. **21**, 222 (2019).

13. F. Aloulou and S. Alila, Int. J. Ind. Chem. **9**, 265 (2018).

14. H. H. Alzoubi, B. A. Albiss, and S. S. Abu sini, Constr. Build. Mater. **236**, 117483 (2020).

15. M. Ahangari and M. Maerefat, Sustain. Cities Soc. **44**, 120 (2019).

16. K. A. R. Ismail and J. N. C. Castro, Int. J. Energy Res. **21**, 1281 (1997).

17. G. Mármol, L. Mattoso, A. C. Correa, C. A. Fioroni, and H. Savastano, J. CO2 Util. **41**, 101236 (2020).

18. A. F. Regin, S. C. Solanki, and J. S. Saini, Renew. Sustain. Energy Rev. **12**, 2438 (2008).

19. F. Aloulou, S. Alila, and H. Sammouda, J. Renew. Mater. **7**, 763 (2019).

20. F. Aloulou, A. Sabrine, and H. Sammouda, J. Renew. Mater. **7**, 631 (2019).

21. D. B. Tripathy, A. Mishra, J. Clark, and T. Farmer, Comptes Rendus Chim. **21**, 112 (2018).

22. H. Bel Hadjltaief, S. Ben Ameur, P. Da Costa, M. Ben Zina, and M. Elena Galvez, Appl. Clay Sci. **152**, 148 (2018).

23. G. Goncalves, P. A. A. P. Marques, R. J. B. Pinto, T. Trindade, and C. P. Neto, Compos. Sci. Technol. **69**, 1051 (2009).

24. P. Yu, Z. Wang, P. Lai, P. Zhang, and J. P. Wang, Constr. Build. Mater. **203**, 356 (2019).

25. I. Msadok, N. Hamdi, M. A. Rodríguez, B. Ferrari, and E. Srasra, Chem. Eng. Res. Des. **153**, 427 (2020).

26. X. Fang and Z. Zhang, Energy Build. **38**, 377 (2006).

27. J. Jeon, J. H. Park, S. Wi, S. Yang, Y. S. Ok, and S. Kim, Chemosphere **236**, (2019).

28. L. Ma, C. Guo, R. Ou, L. Sun, Q. Wang, and L. Li, Energy and Fuels **32**, 5453 (2018).